Applied Clay Science 115 (2015) 30–38

Contents lists available at ScienceDirect

Applied Clay Science

journal homepage: www.elsevier.com/locate/clay

Composition, firing behavior and ceramic properties of the Sejnène clays (Northwest Tunisia)

A. Bennour [a,e], S. Mahmoudi [b,*], E. Srasra [c], S. Boussen [d,e], N. Htira [b,e]

[a] Department of Geology, Faculty of Sciences of Bizerte, Zarzouna 7021, Tunisia
[b] Department of Earth Sciences, Faculty of Sciences of Gabes, Zrig 6072, Tunisia
[c] Laboratory of Physicochemical of Minerals Materials and its Applications National Centre of Research in Materials Sciences BP95, Hammam Lif 2050, Tunisia
[d] Department of Geology, Faculty of Sciences of Tunis, 1060, Belvedere, Tunis, Tunisia
[e] Industrial Rocks and Useful Substances Direction, National Office of Mines, Charguia I, 3023, Tunisia

ARTICLE INFO

Article history:
Received 11 March 2015
Received in revised form 17 June 2015
Accepted 14 July 2015
Available online 23 July 2015

Keywords:
Clay characterization
Firing behavior
Ceramic
Tunisia

ABSTRACT

This study focuses on the results of various analyses and ceramic aptitude tests carried out on two representative clay samples of the Oligo-Miocene from Sejnène, in Northwest Tunisia. The original clays were characterized by chemical analysis, powder X-ray diffraction (XRD), TGA measurements, infrared spectroscopy, Bigot curves and evaluation of the plasticity. The mineralogical study proved that these clays are mainly composed of kaolinite and illite, with a small amount of interstratified I/S. The chemical analysis indicated that the clays of ClaySej1 are more siliceous than those of ClaySej2, which have higher levels of elemental fluxes (Fe_2O_3, Na_2O, K_2O and CaO). The mineralogical metamorphoses during the firing process were recorded via the X-ray diffraction of the raw clays and subsequent firing at 300, 600, 800, 1000 and 1200 °C for 3 h with a heating rate of 10 °C/min. The main transformations were observed at 1000 °C with the appearance of new crystalline phases especially in the ClaySej2 sample. The samples were hand-pressed in a rectangular mold and sintered at 950, 1050 and 1100 °C with a heating rate of 10 °C/min. The variations in flexural strength, linear shrinkage, water absorption and color were also determined and showed sensitivity to the chemical and mineralogical compositions.

1. Introduction

The clays of Tunisia have a wide range of applications mainly in the refractory and ceramic industries. Following the development and mutations that the Tunisian economy has witnessed, there has been insatiable demand for the use of clays in the ceramic industry. Accordingly, in the last few decades many studies have been made on clays and their applications (Khemakhem et al., 2004; Baccour et al., 2008; Felhi et al., 2008; Mohmoudi et al., 2008; Baccour et al., 2009; Hajjaji et al., 2010; Moussi et al., 2011).

Hence, and within this framework, the National Office of Mines undertook the task of compiling an inventory of useful substances across the whole Tunisian soil. The said inventory showed that the country is rich in useful clay substances which stimulated the interest of researchers in studying the most important sites. The Numidian Flysch consists of a thick, turbiditic, sandy and clayey formation of Oligocene–Lower Miocene age which outcrops mainly in northern Tunisia.

The study area is located 12 km northwest of the city of Sejnène and south on the topographic map at 1/50,000 from Cap Negro, between the coordinates UTMC: X = 514672; Y = 4106881. The Sejnène area is characterized by its heavy outcrops of gray clay of the late Oligocene–Miocene (Fig. 1). These clays, with fine sandy layers, occupy the mountain tops of the region (UTMC: Universal Transverse Mercator: Carthage-Tunisia, zone 32).

The present study was carried out in order to characterize two samples of clay: ClaySej1 and ClaySej2. It was collected from sedimentary Oligocene Sejnène deposit, located in Bizerte city (North Tunisia).

Many criteria followed to choose the Sejnène clays for this study as: potential deposits, it's located close to potential urban setting (100 km to the capital) and we can have easy access to the studied zone even in rainy period.

The principal aim of this study is the assessment of potential use of clay deposit in the ceramic industry which will encourage businessmen to invest in this region.

2. Materials and methods

Physical and chemical properties of the samples were investigated by various methods:

The clay fraction was separated by sedimentation technique (Van Olphen, 1963) repeated cation exchange with 1 N NaCl solution. After washing, sedimentation and dialysis, the fine clean sediment was freeze-dried.

* Corresponding author.
E-mail address: salahmahmoudii@yahoo.fr (S. Mahmoudi).

http://dx.doi.org/10.1016/j.clay.2015.07.025
0169-1317/

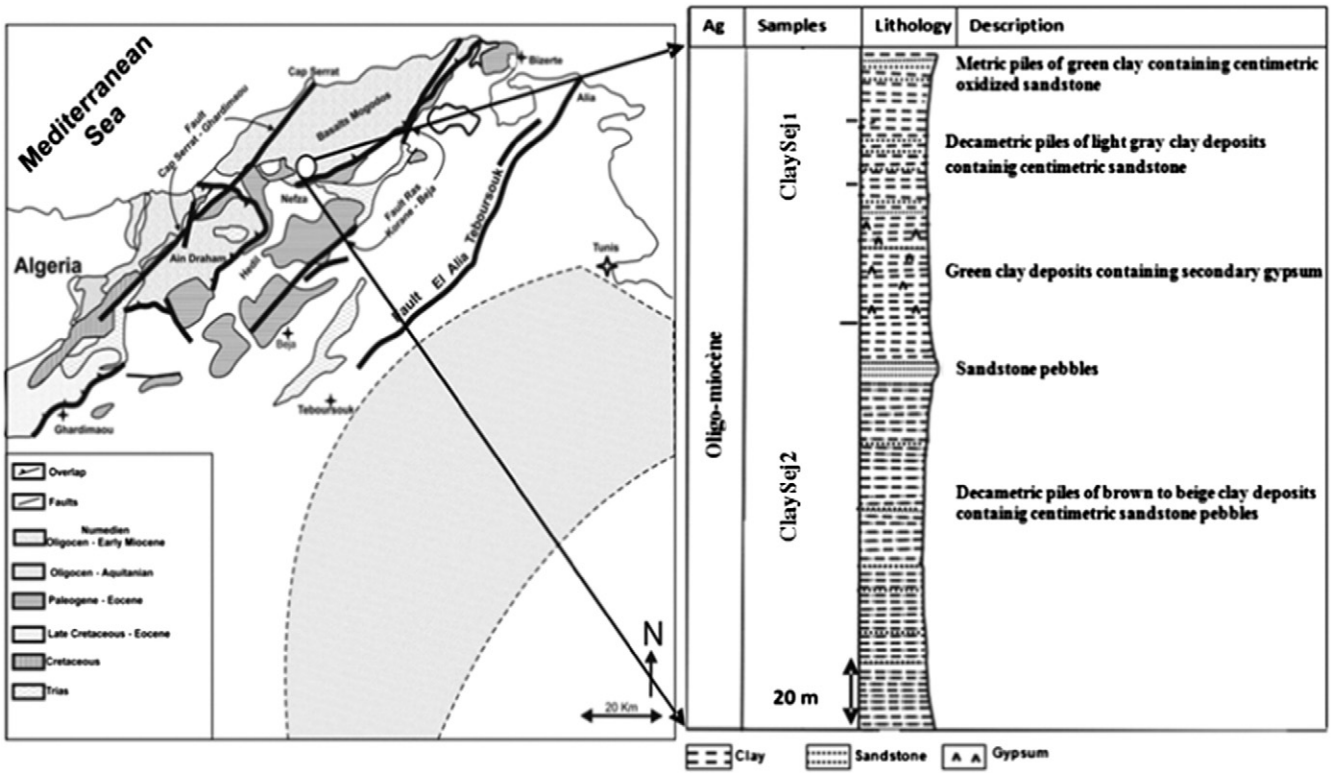

Fig. 1. Location and lithological section of the Sejnène clays.

Mineralogical analysis was performed by X-ray diffraction (XRD) (Philips X'pert equipment with Cu K_α radiation). In this method, oriented specimens are prepared on a glass slide and were left at room temperature. The slides have a density of 2 mg of samples and were successively given treatment: drying at 110 °C, glycosylated for 1 h and heating for 2 h in 500 °C (Bergaya et al., 2006). Diffraction patterns were recorded between 3–60° 2θ at a step size of 0.017° 2θ. The quantification of different phases was carried out using the computer program X'pert High Score. The chemical composition of the samples of ClaySej was obtained by inductively coupled plasma atomic emission (ICP-AES) and mass-spectrometry (ICP-MS) ICP-AES was used to specify Na, K, Ca and Mg, Fe and Si concentration and ICP-MS for Al. This method was carried out following Baccour et al. (2008) methodology. FT-IR spectra were recorded in the region 400–4000 cm^{-1} in an EQUINOX model 55 infrared Fourier transform spectrometer, using the KBr pellet technique (about 2 mg of sample and 200 mg of KBr were used in the preparation of the pellets). The DTA/TG was obtained with a SETRAM type 124. The Casagrande method (LCPC, 1987) was used to measure the consistency limits (Atterberg limits) of the samples of clays. To typify the drying process, the Bigot curves were drawn with an Adamel bare lattograph ADAMEL LHOMARGY, BI, which measures, within 24 h, the change in length and the shape of a slide by adding water to the raw powder until a normal paste that does not stick to fingers is acquired. A sample was used to calibrate the apparatus weighing system. When the sample finished up shrinking, its drying continued at 110 °C. The weight (m) and length (l) of each slide were measured before recording and after complete drying. This method determines graphically the critical point which separates the two drying phases: In the first one, the sample shrinks as it gives off water. In the second phase, the external dimensions of the specimen remain slightly constant in spite of continued water extraction. The ratio ISS was calculated by: ISS (%) = interlayer water (%) / moisture water (%).

Industrial processing:

To simulate industrial pressing conditions, the clays were moistened by sufficient hand mix. They were sieved to pass through (1 mm) until homogeneous agglomerates with 7% of water were obtained (standard ISO, 13006, 1998). They were pressed (250 bar, 70 * 40 * 5 mm) by using a laboratory press. The bodies were dried overnight at 110 °C and were then fired at 950, 1050 and 1100 °C. The typically chosen temperature is that of industrial ceramic faience. For obtained ceramic materials, the following physical parameters were measured: The linear firing shrinkage was evaluated using the formula: ((Id − If) / Id) * 100, where Id and If are the measured lengths of dried and fired samples (standard ISO, 10545-4, 2004).

Table 1
Chemical analysis (%) of the bulk (b) and purified (b) samples.

Sample	L.O.I.	CaO	MgO	SiO_2	Fe_2O_3	Al_2O_3	Na_2O	K_2O	SO_3	TiO_2	MnO	Total
ClaySej1 b	9.58	0.09	0.59	63.03	2.7	19.4	2.53	1.45	0.11	0.21	0.01	99.69
ClaySej1 p	12.95	0.04	0.77	57.53	2.92	23.46	0.15	1.49	<0.01	0.3	0.02	99.63
ClaySej2 b	15.61	4.98	1.47	47.89	8.6	17.68	0.29	1.97	0.36	0.14	0.02	98.99
ClaySej2 p	14.48	2.07	1.33	52.67	5.69	20.20	0.12	2.27	<0.01	0.15	0.03	99.01

Table 2
Minerals estimated by X-ray diffraction.

	Mineralogical compositions (±3%) of the raw materials					
	Quartz	Calcite	Feldspar	Kaolinite	Illite	Illite/smectite
ClaySej1	46	–	3	34	17	–
ClaySej2	20	15	–	27	35	3

Loss on ignition = (weight of specimens before sintering − weight of specimens after sintering) / weight of specimens before sintering.

The average bending strength of 10 specimens was measured with a three point flexural method according to the norm ISO, 10545-4, 2004. It was calculated by: $\sigma f = 3FL / 2bh^2$.

In which F = breaking load (in kg), L = distance between supports, b = sample width and h = sample thickness (all in mm). Each value represents the average of measurements made on ten individual specimens.

The water absorption values, determined according to the AFNOR EN 99, 1982 standard, were calculated from weight differences between the as-fired and water saturated samples (immersed in boiling water for 24 h).

3. Results and discussion

3.1. Chemical analysis

The mass ratio SiO_2/Al_2O_3 is higher for ClaySej1 (3.24%) compared with the ClaySej2 (2.70%), which also indicate a large amount of quartz in the ClaySej1 (Table 1).

Unlike the ClaySej2, the ClaySej1 are still rich in Fe_2O_3 even after purification, probably indicating that the iron is continuously present throughout the crystal lattice.

The CaO content in the purified sample is significantly reduced, implying that the main part of all the calcium in the raw clay stems from the carbonate (Nahdi et al., 2001; Escalera et al., 2014).

3.2. X ray diffraction

The results of all the minerals estimated through X-ray diffraction are given in Table 2.

The nature of the impurities was determined by studying the crude samples (Figs. 2 and 3); quartz is the dominant impurity (101 reflection at 3.34 Å), all the more so for the ClaySej1 sample with a small amount of feldspar. The ClaySej2 sample contains quartz and calcite (reflection at 3.03 Å).

The following mineralogical components were identified in the purified fraction: illite (ICDD reference pattern: 00-002-0050) with a characteristic reflection at 10 Å, is the principal mineral. The presence of kaolinite (ICDD reference pattern: 00-001-0527) with a reflections at 7.14 Å and 3.57 Å which disappear after heating at 500 °C.

The mineralogical composition is the same in all cases, mainly including kaolinite, illite, quartz, calcite and feldspar (Table 2).

3.3. Infrared spectroscopy

The identification of soil minerals by infrared spectroscopy is greatly promoted by reference to spectra (Farmer, 1968).

The infrared absorption properties of kaolinite or halloysite were established at frequencies of 3685, 3665 and 3615 cm^{-1}. The three highest frequencies arise from the hydroxyl on the surface and the lowest frequency from the inner hydroxyl in the kaolinite or halloysite (Fig. 4).

Illite is hydrous mica and displays a small infrared absorption band at 3685 cm^{-1} and a diffused band at about 3600 cm^{-1}. Illite is quite difficult to identify especially by infrared techniques.

The result of the diagnosis of the IR spectra (Fig. 4) proves that quartz was detected in the crude sample of ClaySej1 at 775 and 800 cm^{-1}. The band at 1430 cm^{-1} indicates the disappearance of carbonate after purification.

In the region between 3500 and 4000 cm^{-1}, the IR spectrum of the ClaySej1 sample shows thin and intense bands whereas the bands of the ClaySej2 are larger and less intense thus proving that the ClaySej1 is better crystallized than the ClaySej2.

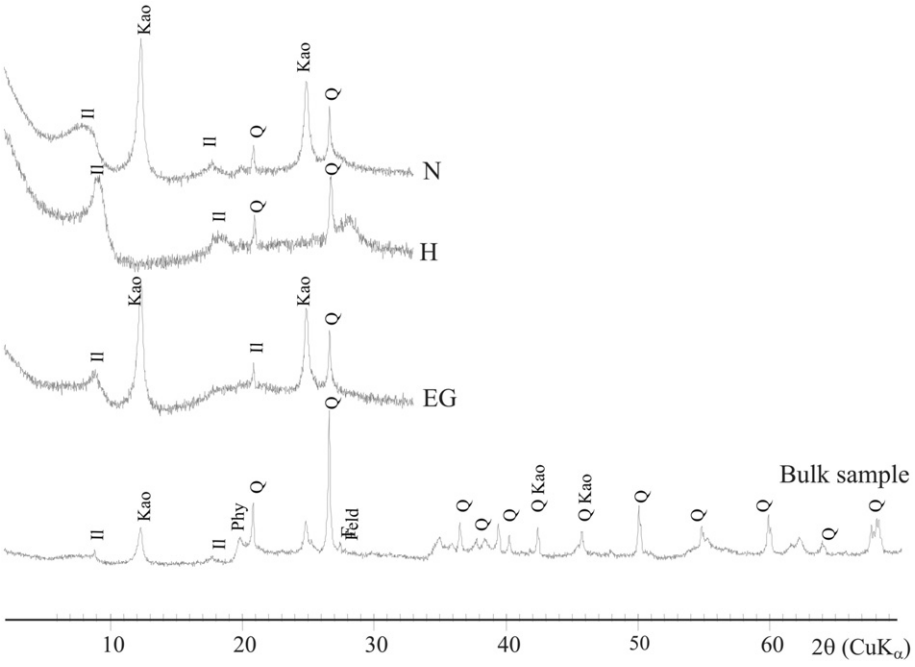

Fig. 2. XRD patterns of the clay fraction of ClaySej1. (N) unprocessed sample; (EG) processed with ethylene glycol; (H) heated at 500 °C and bulk sample. Q: quartz; Il: illite; Kao: kaolinite; Ph: phyllosilicate and Feld: feldspar.

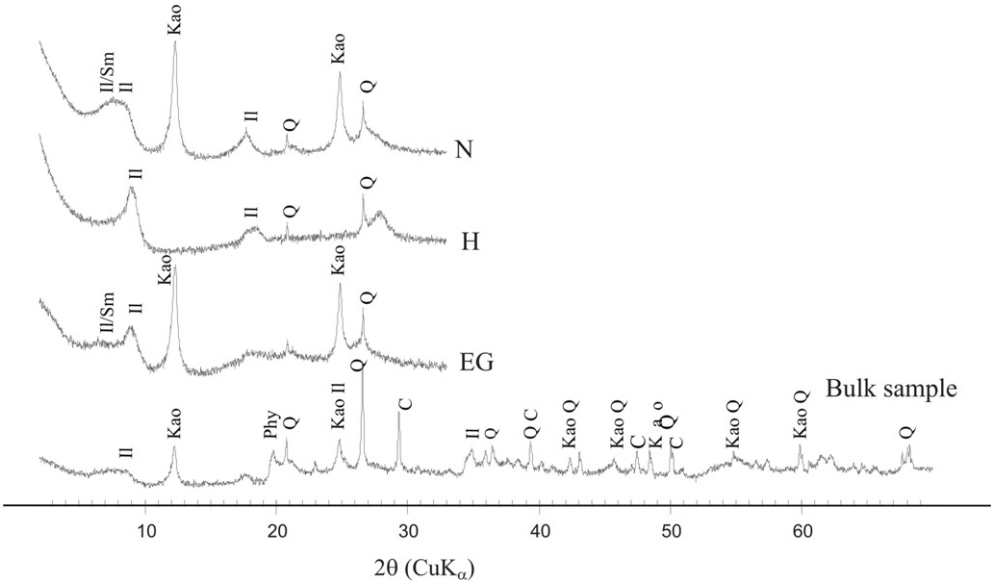

Fig. 3. XRD patterns of the clay fraction of ClaySej2. (N) unprocessed sample; (EG) processed with ethylene glycol; (H) heated at 500 °C and bulk sample. Q: quartz; Il: illite; Kao: kaolinite; Phy: phyllosilicate and C: calcite.

Referring to the IR spectroscopic analysis for kaolinite given by Farmer (1974); Vander Marel and Beutels Pacher (1976), it can be deduced that the ClaySej1 is a well crystallized kaolinite.

3.4. Differential thermal analysis (DTA) and thermo-gravimetry (TG)

The differential thermal analysis (DTA) and thermo-gravimetry (TG) measurements of the ClaySej1 and ClaySej2 are given in Fig. 5. As can be observed in the DTA curves, five consecutive endothermic peaks appeared for all the clays and one exothermic peak for the ClaySej1 sample at 950 °C. These first endothermic peaks were at a temperature lower than 250 °C, proving the removal of weakly-bound water. The peaks of the ClaySej2 at 314 °C and 375 °C show the existence of impurities; while the endothermic peak found at about 488 °C indicates the dehydroxylation of the kaolinite.

The decarbonation reaction of calcite (686 °C) was detected in the structure as well as the formation of quasi-amorphous materials in the ClaySej2 sample.

The total mass loss of the ClaySej1 and ClaySej2 samples was 9.2% and 14.6% respectively (Fig. 5). The greater mass loss for the ClaySej2 compared to that of ClaySej1 is justified by its mineralogical composition and its content of alkaline earth oxides.

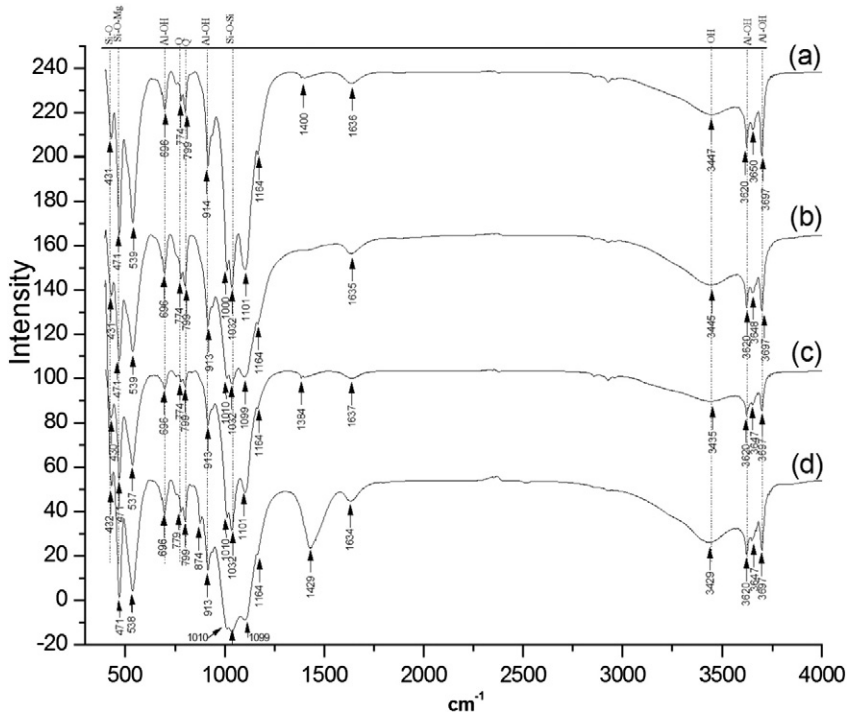

Fig. 4. Infrared spectra of the ClaySej1 (a and b) and ClaySej2 clays (c and d): wavenumber ranging between 400–4000 cm^{-1}.

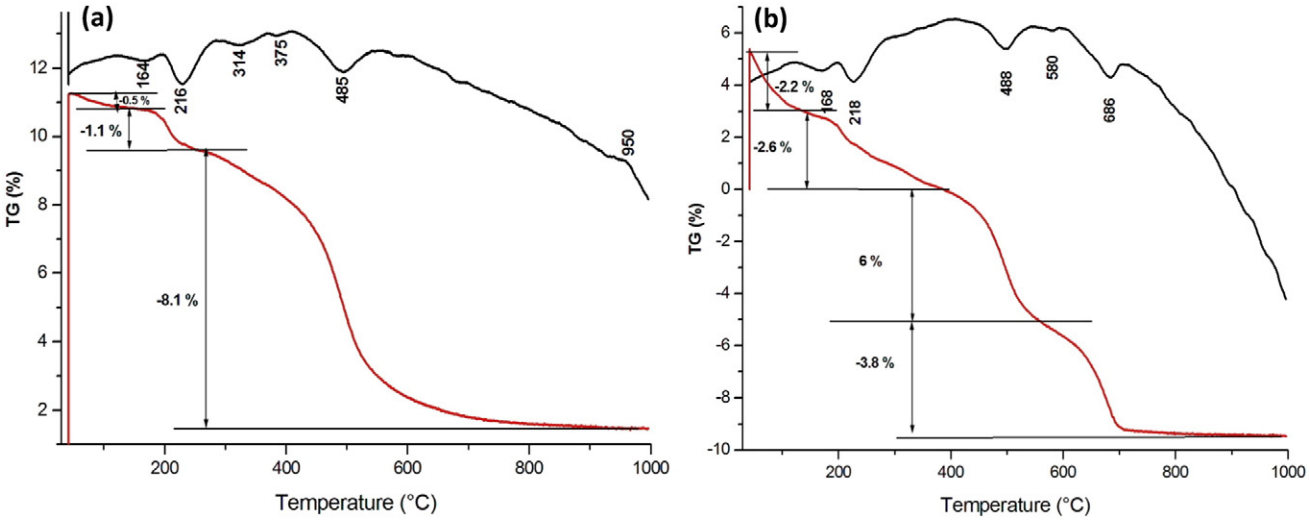

Fig. 5. TGA/TDA curves of the ClaySej1 (a) and ClaySej2 (b) samples.

3.5. Study of the thermal behavior by XRD

The mineralogical mutations during the firing process were analyzed by X-ray diffraction and the X-ray diffractograms of the raw clays after heating at 300, 600, 800, 1000 and 1200 °C for 3 h are given in Figs. 6 and 7.

The mineralogical structure and other physico-chemical properties of various types of clay samples have been extensively studied and discussed in the literature (Moore and Reynolds, 1997; Aras, 2004; Azzouz et al., 2011).

Kaolinite, which is present in both samples, is not subject to the effect of temperatures below 300 °C and disappears completely at a temperature of 600 °C. Illite, on the other hand, gradually decreases until 800 °C. The calcite mineral undergoes the same process as illite. From this temperature on, the destruction of kaolinite coincided with the appearance of an amorphous product which can be metakaolinite (Kakali et al., 2001).

From 1000 °C onwards, remarkable changes have been noticed for the ClaySej2 sample. Accordingly, new phases such as gehlenite, anorthite and hematite appeared. Whereas at this temperature the ClaySej1 sample only contains quartz and feldspar (Figs. 6 and 7).

Hematite (Fe_2O_3) begins to crystallize at 800 °C after the processing of clay minerals and continues to increase until 1200 °C, according to Jordan et al. (1999), Jordan et al. (2001) Manoharan et al. (2011) and Escalera et al. (2014). Thus, it is preferable not to use clays which are rich in iron in ceramics, on the one hand, because it is an unwanted mineral in this industry due to its red color (Stepkowska and Jefferis, 1992) and on the other hand, because it can undergo reactions with the enamel layer to produce an undesirable color.

The gehlenite (2.85 Å) $Ca_2Al_2SiO_7$ and the anorthite $CaAl_2Si_2O_8$ are considered the result of the multistage solid state reactions between the clay matrix and calcite. The gehlenite as unstable intermediate phases in formed from metakaolinite and calcium oxide recorded in the ClaySej2 sample clays which are rich in calcite when processed at

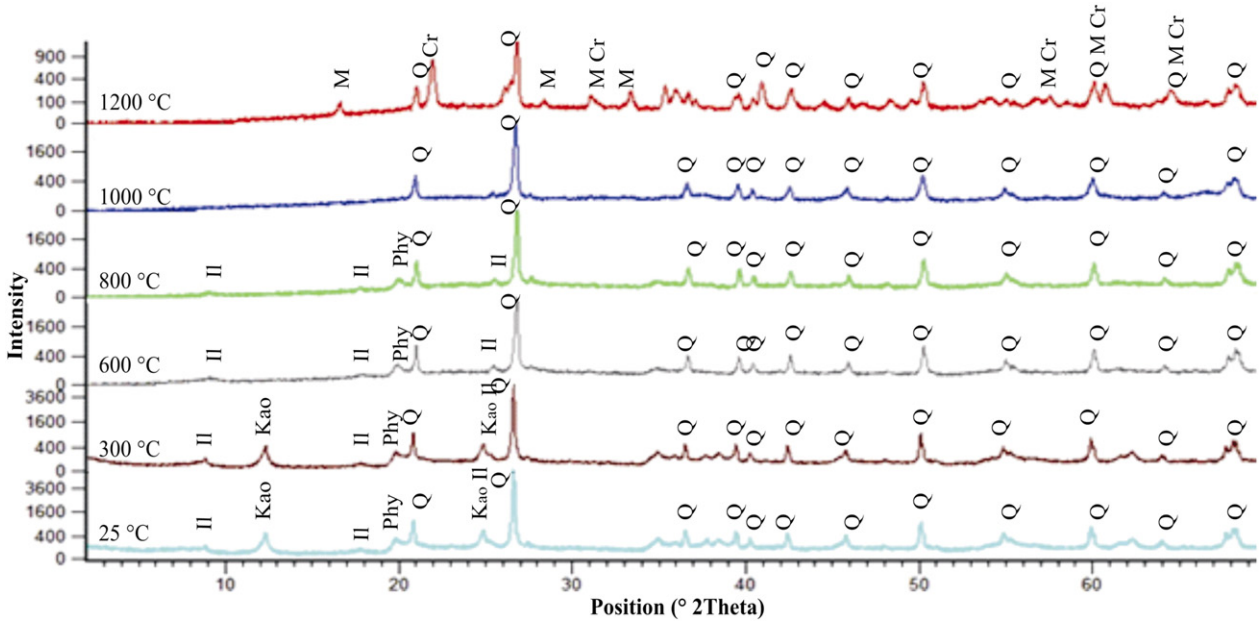

Fig. 6. Powder X-ray diffractograms of the ClaySej1 sample calcined at 300, 600, 800, 1000 and 1200 °C. Reflections in the diffractograms are identified as: Q: quartz; Kao: kaolinite; Il: illite, Felds: feldspar; M: mullite and Cr: cristobalite.

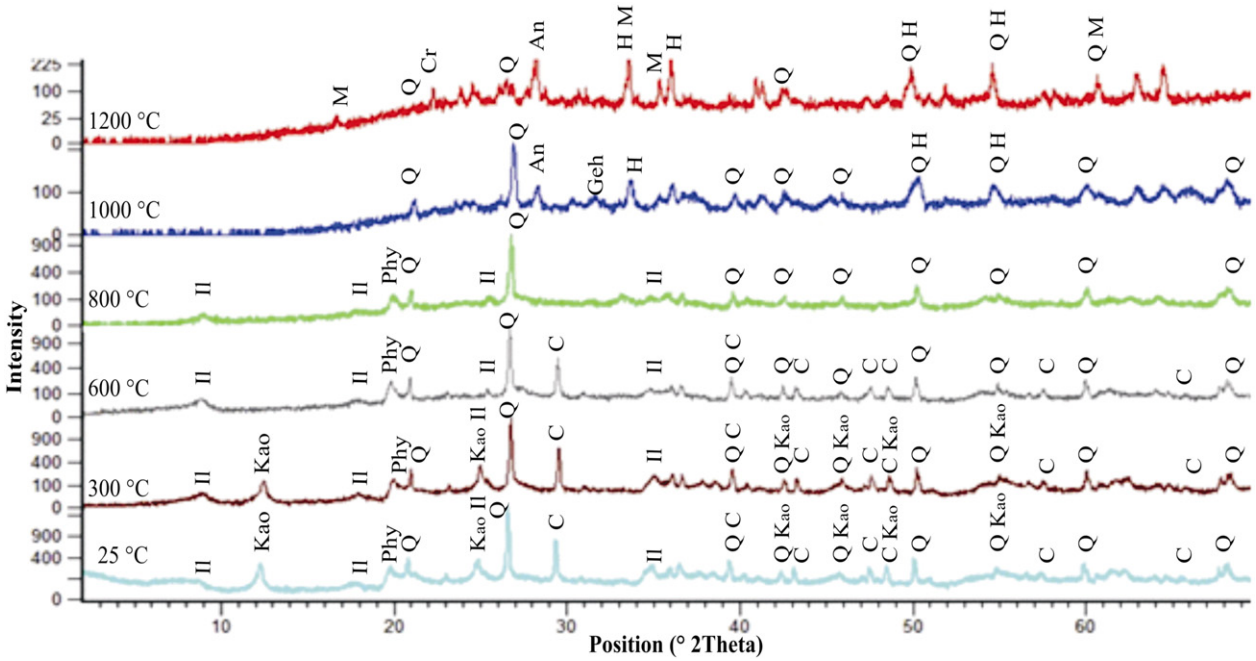

Fig. 7. Powder X-ray diffractograms of the ClaySej2 sample calcined at 300, 600, 800, 1000 and 1200 °C. Reflections in the diffractograms are identified as: Q: quartz; Kao: kaolinite; Il: illite; M: mullite and Cr: cristobalite; C: calcite; H: hematite; Geh: gehlenite and An: anorthite.

1000 °C (Azzouz et al., 2011). In contrary to El-Mahhlawy (2008) and Manoharan et al. (2011), indicating that the presence of anorthite of the fired specimens demonstrated that the firing process reached the equilibrium state; suggesting that the reaction was completed. Anorthite is formed from gehlenite, which is combined with silica and alumina, according to the increase of peak intensity to 1200 °C.

Above 1000 °C, the quartz peak intensity begins to decrease due to the dissolution and to the conversion of a part of SiO_2 in cristobalite.

At 1200 °C mullite, cristobalite and quartz are the only crystalline phases in the ClaySej1 sample while the ClaySej2 sample also contains other minerals such as hematite, gehlenite and anorthite to be used in ceramics and the difference mineral peak intensity were observed (Escalera et al., 2014).

3.6. Assessment of plasticity

In the view of the Holtz and Kovacs diagram, all samples have a sufficient extrudability and a medium plasticity (Fig. 8).

The Atterberg plasticity index indicates that these clays are plastic. The normal plasticity index for ceramic kaolins is about 30–35 (Konta, 1980). The ClaySej1 sample has the optimum molding properties while the ClaySej2 clays have sufficient molding properties. According to the clay workability chart (Fig. 9) of Bain and Highly (1978) they could be used in pottery and bricks (Table 3).

3.7. Bigot curves

The drying capacities given in the Bigot curves (Ratzemberger, 1990) for the analyzed clay deposits were generated by their drying results obtained in a semi-industrial simulation. The Bigot curves (Fig. 10) are used as prime indicators in the selection of raw materials (Ratzemberger, 1990; Dondi et al., 1998; Meseguer, 2010) in the ceramic industry.

The feature of two clay samples (ClaySej1 and ClaySej2) after drying proves that the totals of drying behavior are 23.5% and 25.9% (Table 4). The first mass loss which is associated with shrinkage is characteristically

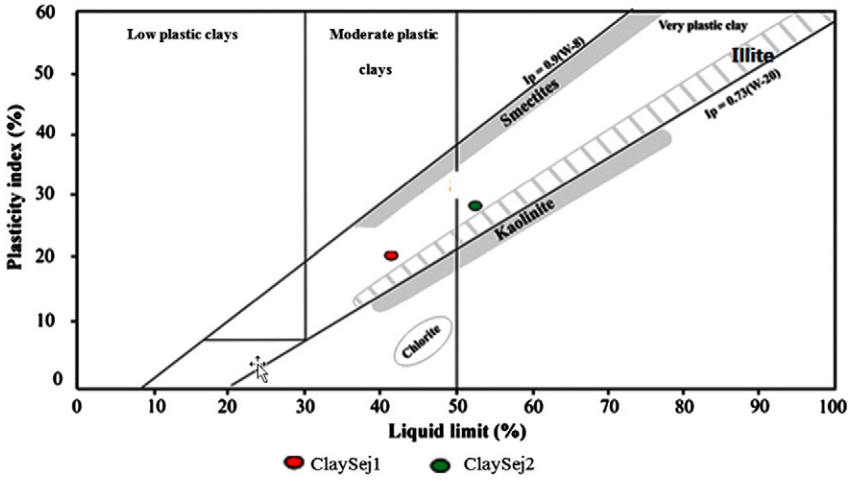

Fig. 8. Position of the studied clays on the Holtz and Kovacs diagram.

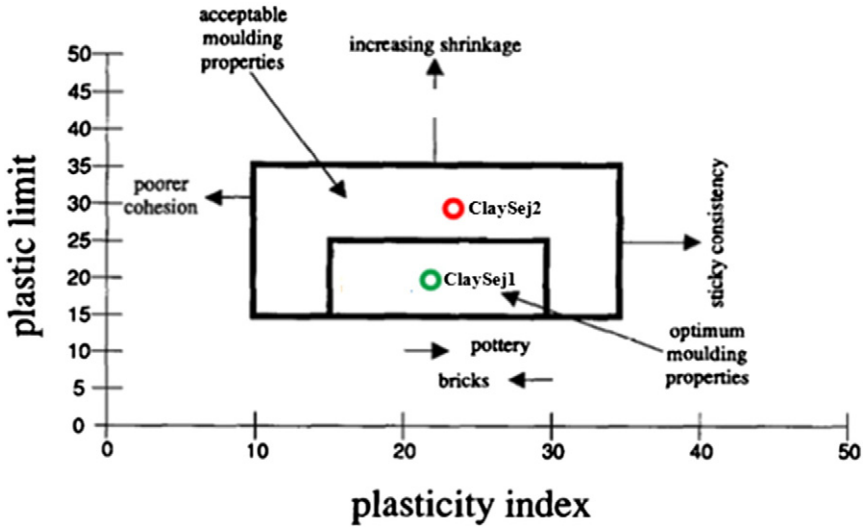

Fig. 9. Clay workability chart.
According to Bain and Highly (1978).

high for the Sejnène clays and it is rated as 22.1% and 19.3% respectively. This loss is characterized by two stages, the first stage with a constant rate at 5.5% for ClaySej1 and 11.3% for ClaySej2. While the second is with a falling rate, it is at 11.6% for ClaySej1 and 8% for ClaySej2 (Table 4). The second mass loss is not associated with further drying shrinkage and is comparatively lower than the first mass and is recorded as 1.4% and 6.6% respectively (Fig. 10).

The present significant variation of the parameters to Bigot curves, indicating that ClaySej1 is a siliceous clay and is characterized by shrinkage while the ClaySej2 is characterized by a slow drying behavior and requiring the addition of a degreaser.

Table 3
Plasticity values (±2%) of the studied samples.

Sample	Liquid limit W_L	Plastic limit Wp	Plasticity index PI
ClaySej1	41	21	20
ClaySej2	52	23	29

3.8. Ceramic tests

In order to obtain high-strength ceramic bodies, absorbed and crystalline water must be removed and a large amount of the glass phase should be formed. To identify the different ceramic body characteristics (sintering shrinkage, loss on ignition, porosity, resistance to bending and color), 1000 °C, 1050 °C and 1100 °C were selected as firing temperatures for the ceramic bodies.

As a result, the increase of these parameters coincided with the rise in the firing temperatures for both types.

3.8.1. Firing shrinkage

The findings of the fired clays, linear firing shrinkage and water absorption are exhibited in Table 5. An increase in the shrinkage is associated with an increase in firing temperature and the greatest tendency was found above 1050 °C.

The firing shrinkage is justified by the amalgamation of cavities and the production of the liquid phase in the product (Monteiro and Vieira, 2004). This result varies for both clays. The sintering shrinkage variation

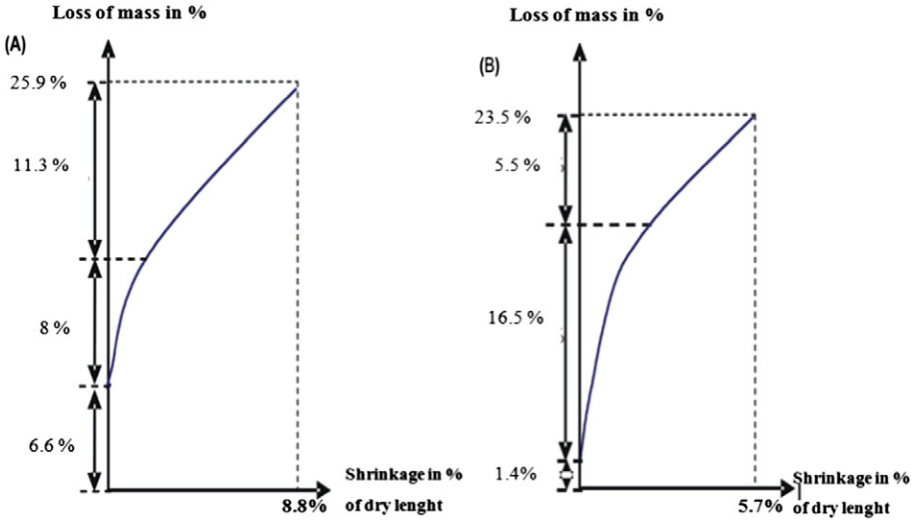

Fig. 10. Bigot curves of the ClaySej1 (B) and ClaySej2 (A) clay minerals.

Table 4
Drying parameters (±2%) from the Bigot curves for the two clay samples.

Sample	Mass loss with shrinkage		Mass loss with no shrinkage	Mass loss	Shrinkage in (%) of dry length
	Constant rate	Failing rate			
ClaySej1	5.5	16.6	14	23.5	5.7
ClaySej2	11.3	8	6.6	25.9	8.8

Table 5
Firing parameters (±1.5%) of two clay samples.

Sample	Temperature (°C)	Water absorption (%)	Loss on ignition (%)	Firing shrinkage (%)	Flexural strength (N/mm^2)
ClaySej1	950	16.6	7.5	1.7	6.8
	1050	14.3	7.8	2.8	11.8
	1100	8	8	5.5	25.1
ClaySej2	950	11	12	4.8	25.3
	1050	8.8	12.3	8.3	30.1
	1100	5.8	12.4	8.5	31.4

(Table 5) is very important for the ClaySej2 in the interval 950 to 1050 °C; for the ClaySej1 this interval happens between 1050 °C and 1100 °C due to the siliceous nature of these clays (Ngun, 2011).

3.8.2. Loss on ignition

The loss on ignition of the ceramic bodies increased with the firing temperature (Table 5). The maximum variation of this characteristic was recorded at a temperature lower than 950 °C. This parameter slightly varies between 950 °C and 1100 °C. This variation precludes that the volatile components contributing to the loss on ignition had been removed or decomposed at temperatures below 950 °C. In many previous studies (Rankin et al., 1987; Nahdi et al., 2001) have proven that 1000 °C is the maximum temperature for the total loss on ignition (Table 1) which correlates with the findings of the present paper. Indeed, the ClaySej2 sample presents a higher loss on ignition than the ClaySej1 sample during the decomposition of calcite, the removal of absorbed and crystalline water and the release of CO_2; confirming the data obtained from the chemical and mineralogical analyses, which highlights the importance of the impurities percentage in the ClaySej2.

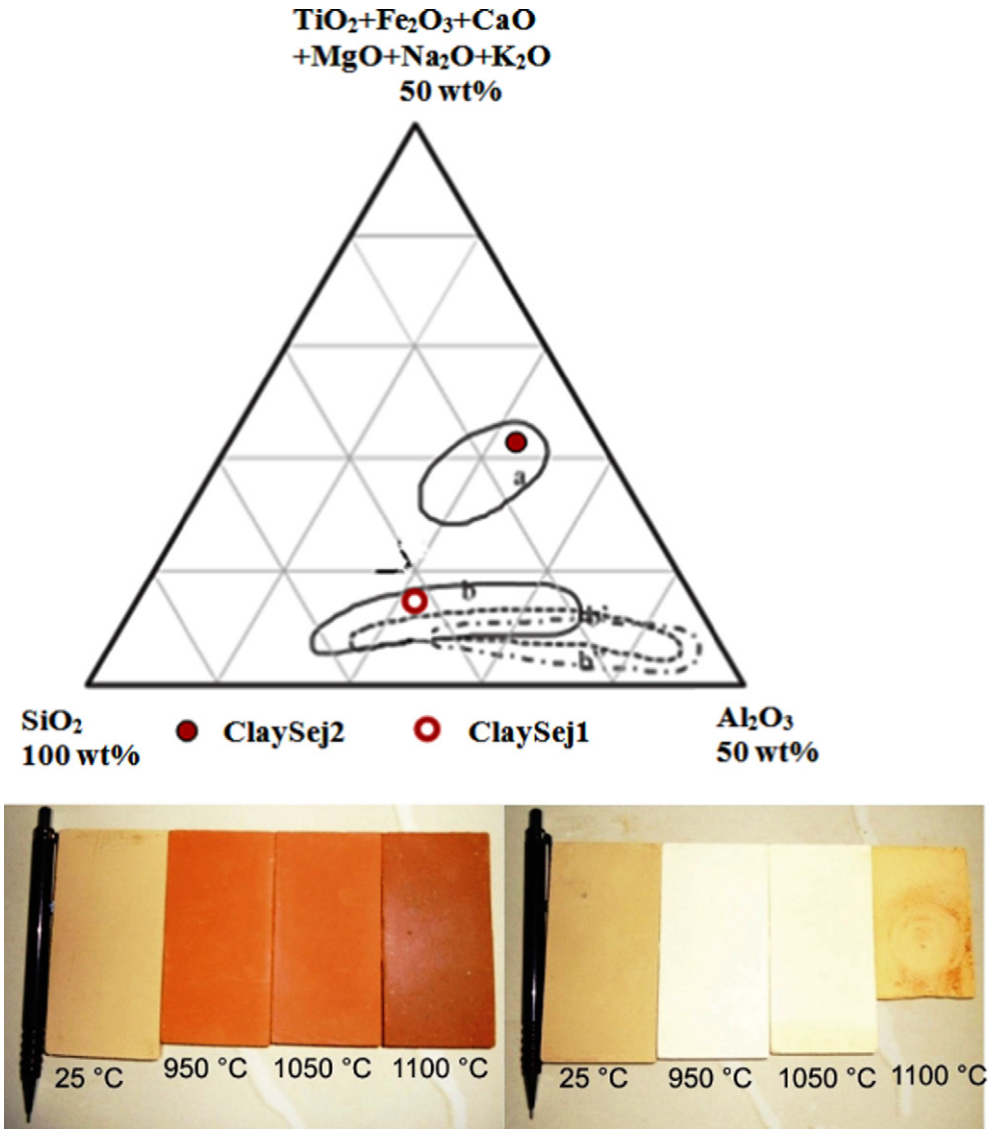

Fig. 11. (a): Triangular diagram of Sejnène clays: SiO_2/Al_2O_3/other oxides. a = red stoneware (Italy); b, b′, b* = white stoneware for German, English and French industries, respectively (data from Fabbri and Fiori, 1985), (b): Ceramic bodies fired at different temperatures.

3.8.3. Bending strength and porosity tests

The porosity variation and the mechanical resistance to the inflection were calculated at different temperatures (Table 5).

An increase in the flexural strength was noticed in the two samples and this was related to the increase in the firing temperature and to the porosity reduction. This increase for the ClaySej1 sample presents a very pronounced slope of the straight line which joins the point corresponding to 1050 °C with the point at 1100 °C. While for the ClaySej2, this variation was more important starting from 950 °C with a slight increase up to 1100 °C.

Generally, raw materials for ceramic pastes containing $CaCO_3$ and alumina silicates are liable to form crystalline phases at relatively low temperatures from 950 °C to 1000 °C (Kamsen and Leonelli, 2007; Alcântara et al., 2008). Consequently, at 950 °C the porosity gradually decreases for the ClaySej2 sample, coinciding with the inception of vitrification. However, this gradual decrease in porosity happens in the temperature interval between 1050 °C and 1100 °C for the ClaySej1 sample.

3.8.4. Color

The ceramic wares coloration can be appreciably modified due to the presence of Fe_2O_3 as well as other constituents such as CaO, MgO, MnO and TiO_2 (Kreimeyer, 1987). Previous studies (Fabbri and Fiori, 1985) identified the different clays' quality from the percentage of their components.

At a temperature of 1100 °C, the ClaySej2 has a red brick color because of the presence of a higher percentage of Fe_2O_3 (8.6%), while that of ClaySej1 is of a beige-cream color (Fe_2O_3 = 2.7%). These results coincide with the premises of (Murray, 2007) who argued that the clays which contain 5% or more of Fe_2O_3 are red-firing clays; while others which contain between 1 and 5% of Fe_2O_3 are B tan-burning clays; and yet others which contain less than 1% of Fe_2O_3 are white-firing clays (Fig. 11). Therefore, they cannot be used for the production of fine ceramics, however, they could be considered as raw materials for structural ceramic products (Konta, 1995).

4. Conclusion

The study of two Sejnène clays with distinct chemical compositions indicated that the ClaySej1 are rich in silica with a low content of alkali elements unlike the ClaySej2. The flux elements such as (Fe_2O_3, MgO, K_2O and Na_2O) have a considerable effect on the thermal behavior and properties of the final ceramic products.

The wealth of iron sample after purification indicates the iron is continuously present throughout the crystal lattice. The ceramic behaviors of the ClaySej were interpreted by linear firing shrinkage, water absorption and flexural strength. The change of various parameters in the ClaySej2 occurs in the temperature interval between 950 and 1050 °C; while for the ClaySej1 the significant changes take place at a temperature above 1000 °C.

The mineralogical transformations during the firing process were analyzed by X-ray diffraction and indicated that the main observed mutation for the ClaySej2 sample led to the emergence of new phases at 1000 °C.

Remarkable changes were observed for the ClaySej2 sample which led to the appearance of new phases namely gehlenite, anorthite and hematite; while quartz and feldspar were observed in the ClaySej1 sample due to its low impurity content.

References

AFNOR EN 99, 1982. Carreaux et dalles céramiques. Détermination de l'absorption d'eau (6 pp.).

Alcântara, A., Beltrão, M.S.S., Oliveira, H.A., Gimenez, I.F., Barreto, L.S., 2008. Characterization of ceramic tiles prepared from two clays from Sergipe — Brazil. Appl. Clay Sci. 39, 160–165.

Aras, A., 2004. The change pf phase composition in kaolinite and illite rich clay based ceramic bodies. Appl. Clay Sci. 24, 257–269.

Azzouz, H., Alouani, R., Saïd Tlig, S., 2011. Mineralogical characterization of ceramic tiles prepared by a mixture of Cretaceous and Mio-Pliocene clays from Tunisia: factory and laboratory product. Ceram. Soc. Jpn. 119, 93–100.

Baccour, H., Medhioub, M., Jamoussi, F., Mhiri, T., Daoud, A., 2008. Mineralogical evaluation and industrial applications of the Triassic clay deposits, Southern Tunisia. Mater. Charact. 59, 1613–1622.

Baccour, H., Medhi, M., Jamoussi, F., Mhiri, T., 2009. Influence of firing temperature on the ceramic properties of Triassic clays from Tunisia. J. Mater. Process. Technol. 209, 2812–2817.

Bain, J.A., Highly, D.E., 1978. Regional appraisal of clay resources challenge to the clay mineralogist. In: Mortland, M.M., Faxmer, V.C. (Eds.), Proc. Int. Clay. Conf.Elsevier, Amsterdam, pp. 437–446

Bergaya, F., Theng, B.K.G., Lagaly, G., 2006. Developments in clay science. Handbook of Clay Science 1. Elsevier, Amsterdam (1248 pp.).

Dondi, M., Marsigli, M., Ventura, I., 1998. Sensibilità all'es siccamento e caratteristiche porosimetriche delle argille italiane per laterizi. Ceramurgia 28, 1–8.

El-Mahhlawy, M., 2008. Characteristics of acid resisting bricks made from quarry residues and waste steel slag. Constr. Build. Mater. 228, 1887–1896.

Escalera, E., Tegman, R., Marta-Lena Antti, M.L., Odén, M., 2014. High temperature phase evolution of Bolivian kaolinitic–illitic clays heated to 1250 °C. Appl. Clay Sci. 101, 100–105.

Fabbri, B., Fiori, C., 1985. Clays and complementary raw materials for stoneware tiles. Mineral. Petrogr. Acta 535–545.

Farmer, V.C., 1968. Infrared spectroscopy in clay minerals study. Clay Miner. 7, 373–387.

Farmer, V.C., 1974. The infrared spectra of minerals. Mineral. Soc. 331–365.

Felhi, M., Tlili, A., Gaied, M.E., Montacer, M., 2008. Mineralogical study of kaolinitic clays from Sidi El Bader in the far north of Tunisia. Appl. Clay Sci. 3 (4), 208–217.

Hajjaji, W., Hachani, M., Moussi, B., Jeridi, K., Medhioub, M., López-Galindo, A., Rocha, F., Labrincha, J.A., Jamoussi, F., 2010. Mineralogy plasticity clay sediments north east Tunisia. J. Afr. Earth Sci. 57, 41–46.

ISO 10545-4, 2004. Ceramic tiles. Part 4: Determination of Modulus of Rupture and Breaking Strength edition 2.

ISO 13006, 1998. Ceramic tiles. Definitions, Classification, Characteristics and Marking edition 1.

Jordan, M.M., Boix, A., Sanfeliu, T., De la Fuente, C., 1999. Firing transformations of Cretaceous clays used in the manufacturing of ceramic tiles. Appl. Clay Sci. 14, 225–234.

Jordan, M.M., Sanfeliu, T., De la Fuente, C., 2001. Firing transformations of Tertiary clays used in the manufacturing of ceramic tile bodies. Appl. Clay Sci. 20, 87–95.

Kakali, G., Perraki, T., Tsivilis, S., Badogiannis, E., 2001. Thermal treatment of kaolin: the effect of mineralogy on the pozzolanic activity. Appl. Clay Sci. 20, 73–80.

Kamsen, E., Leonelli, C., 2007. Non-contact dilatometry of hard and soft porcelain compositions. J. Therm. Anal. Calorim. 88 (2), 571–576.

Khemakhem, S.R., Amar, Ben, Ben Hassen, R., Larbot, A., Ben Salah, A., Cot, L., 2004. Production of tubular ceramic membranes for microfiltration and ultrafiltration. Ind. Ceram. 24 (3), 117–120.

Konta, J., 1980. Properties of ceramic raw materials. Ceramic MonographsHandbook of CeramicsSchmid, Freiburg, pp. l–32.

Konta, J., 1995. Clay and man: clay raw materials in the service of man. Appl. Clay Sci. 10, 271–273.

Kreimeyer, R., 1987. Some notes on the firing color of clay bricks. Appl. Clay Sci. 2, 175–183.

LCPC, 1987. Limites d'Atterberg, limite de liquidité, limite de plasticité. Méthode d'essai n°19. Laboratoire Central des Ponts et Chaussées (26 pp.).

Manoharan, C., Sutharsan, P., Dhanapandian, S., Venkatachalapathy, R., Mohamed Asanulla, R., 2011. Analysis of temperature effect on ceramic brick production from alluvial deposits, Tamilnadu, India. Appl. Clay Sci. 54, 20–25.

Meseguer, S., 2010. Ceramic behaviour of five Chilean clays which can be used in the manufacture of ceramic tile bodies. Appl. Clay Sci. 47, 372–377.

Mohmoudi, S., Srasra, E., Zargouni, F., 2008. The use of Tunisian Barremian clay in the traditional ceramic industry: optimization of ceramic properties. Appl. Clay Sci. 42, 125–129.

Monteiro, S.N., Vieira, C.M.F., 2004. Influence of firing temperature on the ceramic properties of clays from Campos dos Goytacazes, Brazil. Appl. Clay Sci. 27, 229–234.

Moore, D.M., Reynolds Jr., R.C., 1997. X-ray Diffraction and the Identification and Analysis of Clay Minerals. 2nd ed. Oxford University Press (400 pp.).

Moussi, B., Medhioub, M., Hatira, N., Yans, J., Hajjaj, W., Rocha, F., Labrincha, J.A., Jamoussi, F., 2011. Identification and use of white clayey deposits from the area of Tamra (northern Tunisia) as ceramic raw materials. Clay Miner. 46, 165–175.

Murray, H.H., 2007. Applied clay mineralogy. Developments in Clay Science 2. Elsevier B.V

Nahdi, K., Gasmi, N., Trabelsi Ayedi, M., Kbir-Ariguib, N., 2001. Characterization and thermal behaviour of Jebel Ressas clay. J. Soc. Chim. Tunis. 4, 1125–1134.

Ngun, B.K., 2011. Some ceramic properties of clays from central Cambodia. Appl. Clay Sci. 53, 33–41.

Rankin, A.H., Miller, M.F., Carter, J.S., 1987. The release of trace elements and volatiles from crinoidal limestone during thermal decrepitation. Mineral. Mag. 51, 517–525.

Ratzemberger, H., 1990. An accelerated method for the determination of drying sensitivity. Ziegelind. Int. 43, 348–354.

Stepkowska, E.T., Jefferis, S.A., 1992. Influence of microstructure on firing colour of clays. Appl. Clay Sci. 6, 319–342.

Van Olphen, H., 1963. An Introduction to Clay Colloid Chemistry. Interscience Publishers, New York.

Vander Marel, H.W., Beutels Pacher, H., 1976. Atlas Infrared Spectroscopy of Clay Minerals and Their Admixtures. Elsevier Scientific Publishing Company.